Available online at www.sciencedirect.com

SCIENCE DIRECT®

Catalysis Today 98 (2004) 115–121

CATALYSIS TODAY

www.elsevier.com/locate/cattod

Characterization of hydrothermally treated MCM-41 and Ti-MCM-41 molecular sieves

P. Schacht[a,b,*], L. Noreña-Franco[b], J. Ancheyta[a], S. Ramírez[a], I. Hernández-Pérez[b], L.A. García[a]

[a]*Instituto Mexicano del Petróleo, Eje Central Lázaro Cárdenas No. 152, México, DF 07730, México*
[b]*Universidad Autónoma Metropolitana Azcapotzalco, Av. San Pablo 180, México, DF 02200, México*

Abstract

In this work we report the characterization and results of hydrothermal treatment tests performed on MCM-41 and Ti-MCM-41 materials at two temperatures, 450 and 550 °C. Based on BET analyses and XRD measurements, results showed a decrease in specific surface area, pore volume and pore size for both materials after the hydrothermal treatments. The Ti-MCM-41 material was more stable than the MCM-41. The specific surface area reduction for the hydrothermally treated Ti-MCM-41 samples at 450 and 550 °C was 16% and 29%, respectively. Similarly, there was a reduction of the interplanar spacing of 30% and 33%, respectively, observed as a displacement of the main diffraction peak towards larger diffraction angles. We also report the conversion and selectivity of these materials in the HDS reaction of DBT. A higher conversion was obtained with the Ti-MCM-41 supported catalyst.

Keywords: Hydrothermal treatment; HDS; Catalytic supports; Ti-MCM-41

1. Introduction

Hydrodesulfurization (HDS) is one of the most important processes in the modern oil refining industry. The HDS process is widely used for improving the quality of petroleum distillates. However, due to new specifications of fuels, such as diesel, this process faces an enormous challenge, since sulfur compounds present in this type of distillates are more difficult to remove. The more refractory to HDS sulfur compounds are well known to be 4-methyl DBT and 4,6-dimethyl DBT, which contain side chains in positions that limit the access of the molecule to the active sites of the catalyst [1,2]. To achieve the ultra-low sulfur contents required in future diesel fuels, i.e. 10–30 wppm, activity of the catalyst must be enhanced.

The support has a fundamental role in determining the nature, number of active sites and the activity of the catalyst. During many years γ-Al_2O_3 has been the traditional support for HDS catalyst with large commercial application. Other supports have also been reported in the literature to be attractive for HDS catalysts, such as TiO_2, ZrO_2, SiO_2, mixed oxides, among others. However, it is necessary to explore and develop better materials for supporting active components such as Co, Mo or Ni.

It is well known that MCM-41 materials possess a porous system consisting of a hexagonal array of channels with diameters varying from 15 to 100 Å [3,4]. It has also been found that MCM-41 has good thermal stability in air and water vapor hydrothermal treatments [3,5,6]. However, the mesoporous structure of MCM-41 may collapse in hot water and in aqueous solution due to hydrolysis reactions [5,6]. An improvement of thermal and hydrothermal stability when incorporating La^{3+} and Fe^{3+} in the MCM-41 framework has been reported in the literature [7,8]. Based on X-ray diffraction and infrared spectroscopy data He et al. [9] explained such behavior of Fe and La containing materials, suggesting that it was due to the increase of the wall thickness of the mesoporous channels and to the reduction of the number of aluminium vacancies.

The main objective of this paper is to study the effect of the incorporation of Ti into the MCM-41 structure on the

---

* Corresponding author.
E-mail address: pschacha@imp.mx (P. Schacht).

0920-5861/$ – see front matter © 2004 Elsevier B.V. All rights reserved.
doi:10.1016/j.cattod.2004.07.057

hydrothermal stability of the support as well as compare the changes in crystalline structure with MCM-41 prepared by the same procedure. Thermogravimetric analysis, BET analysis, X-ray diffraction, infrared spectrometry and transmission electronic microscopy techniques were employed for the materials characterization.

2. Experimental

2.1. Synthesis

The Ti-containing MCM-41 samples were synthesized by a direct hydrothermal method using cetyltrimethylammonium chloride, tetrabuthylammonium hydroxide, fumed silica and titanium (IV) ethoxide as titanium source, all supplied by Aldrich. The formulation was modified according to a procedure previously reported [10,11] keeping a organic component/(SiO_2 + TiO_2) molar ratio of 0.35 and a SiO_2/TiO_2 molar ratio of 25. The nominal Ti content was 3% w/w. The mixture was transferred to a Teflon bottle and placed in an autoclave at 110 °C for 48 h. The solid product was recovered by filtration, washed with doubly deionized water, and dried at room temperature. Finally, the material was calcined at 540 °C for 6 h.

2.2. Hydrothermal treatment

The hydrothermal stability of the materials was studied at temperatures of 450 and 550 °C in a quartz reactor. The system is fitted with temperature control, an air-flow system and a water vapor generator. First, the samples were heated under dry airflow from room temperature to 200 °C and maintained at this temperature for 1 h. Afterwards, the samples were heated from 200 to 450 °C (5 °C/min) under air saturated with water vapor and maintained at 450 °C for 2 h. A similar procedure was carried out for testing the hydrothermal stability at 550 °C. The samples were labeled as Ti-MCM-41 (450), Ti-MCM-41 (550), MCM-41 (450), and MCM-41 (550). The number inside parenthesis indicates the treatment temperature.

2.3. Characterization

The specific surface area of the samples was determined by means of the BET method, using a Micromeritics ASAP 2000 sorptmeter. X-ray diffraction (XRD) spectra were recorded employing a Siemens D-5000 instrument fitted with a monochromator for Cu Kα radiation operating at 40 kV, 40 mA. A Nicolet 7000 FT-IR Spectrophotometer with a quartz cell was used for infrared spectrometry. Thermogravimetric analyses (TGA) were obtained with a Perkin-Elmer 1700 and micrographs with a JEOL 100CX TEM.

2.4. Activity tests

Activity tests were carried out in a Parr batch reactor. For each experiment, 240 mg of catalyst were loaded into the reactor. Before the HDS reaction, the catalysts were sulfided with a mixture of H_2/H_2S (10/90 vol.%) at 400 °C during 1 h. DBT hydrodesulfurization was chosen as catalytic activity test. The reaction was carried out at the following operating conditions: 300 °C reaction temperature, 400 psig pressure, 6.3 mol/mol hydrogen-to-oil ratio, during 6 h. The reaction mixture consisted of DBT and hexadecane as solvent (0.5 wt.% sulfur as DBT).

Product analyses were performed on-line in a Perkin-Elmer chromatograph equipped with a 50 m HP Ultra 2 capillary column with a flame ionization detector (FID).

Conversion in each experiment was defined as 100 minus unconverted DBT in weight percent, and product selectivity was calculated by dividing product yield and conversion.

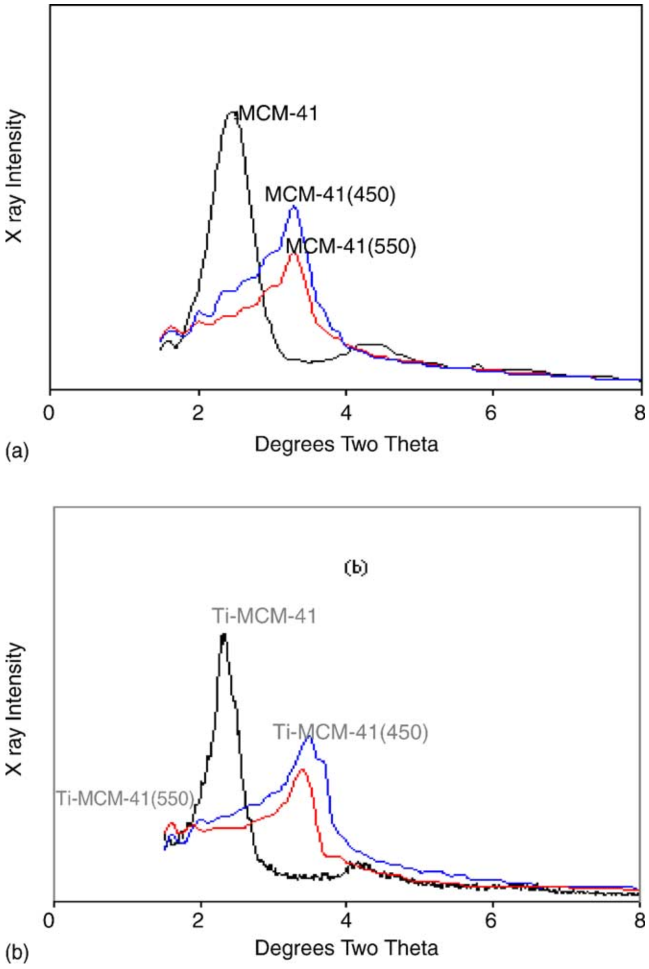

Fig. 1. X-ray powder diffraction patterns of MCM-41 (a) and Ti-MCM-41 (b) before and after hydrothermal treatment.

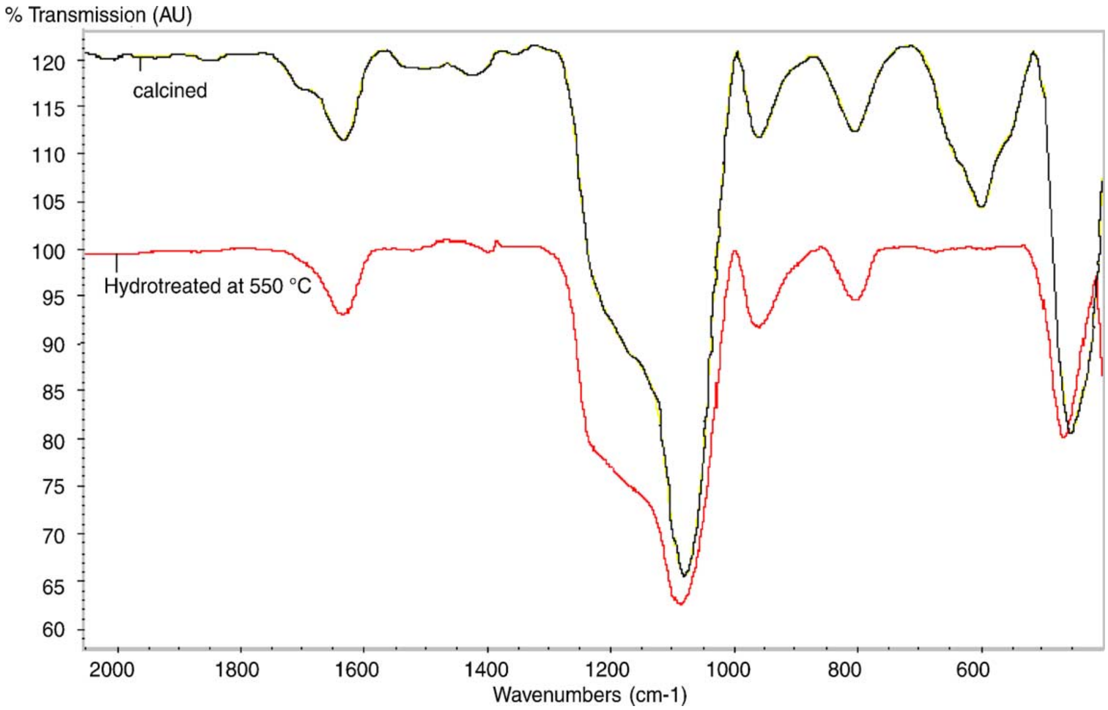

Fig. 2. FT-IR of Ti-MCM-41.

3. Results and discussion

3.1. X-ray diffraction

Fig. 1 presents the powder X-ray diffractograms of the calcined samples. It can be seen that all calcined samples show the typical XRD pattern of MCM-41 with a well-defined (1 0 0) reflection peak, as described by Beck [3,4]. The diffraction pattern of the material containing Ti indicates that the metalosilicate, like the pure MCM-41, has an ordered structure of a hexagonal pore array. In the case of Ti containing MCM-41 prepared by direct synthesis, the introduction of Ti had a small effect on the formation of the mesoporous structure.

The XRD patterns of MCM-41 and Ti-MCM-41 after thermal treatment at 450 and 550 °C are also shown in Fig. 1. The main peak of each sample becomes less intense and wider, indicating more degree of disorder. There is also a displacement of the main peak towards a larger diffraction angle, indicating a reduction of the cell parameter. The secondary peaks cannot be observed, which are also related to a less regular structure. For the Ti-MCM-41 material after hydrothermal treatment, the main diffraction peak was displaced from a diffraction angle of 2.5–3.5θ, corresponding to a 30% and 33% smaller interplanar spacing, respectively.

3.2. FT-IR

The infrared spectra of the Ti-MCM-41 sample before and after hydrothermal treatment at 550 °C (Fig. 2), showed an absorption band at approximately 953 cm^{-1}, which is commonly associated to tetrahedral Ti, integrated into the framework [12,13]. This absorption band is sometimes associated to silanol groups perturbed by neighbouring metal ions, such as Ti ions. It indicates that the titanium remains part of the framework after the hydrothermal treatment. The other main peaks are: a characteristic broad band centered at approximately 3740 cm^{-1} associated to OH from the silanol group (not shown), overlapped by hydration water; two bands (1234 and 1098 cm^{-1}) associated to Si–O–Si asymmetric vibrational stretching; a band at approxi-

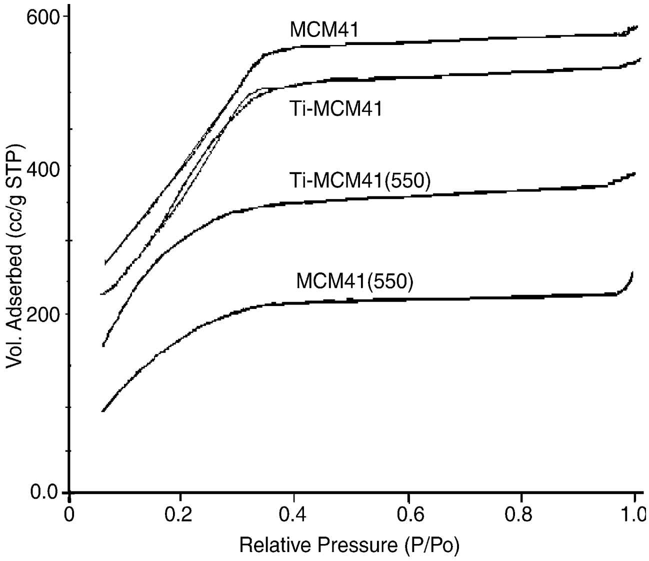

Fig. 3. BET behavior of MCM-41 and Ti-MCM-41 before and after hydrothermal treatment.

mately 1628 cm^{-1} associated to Ti–O–Si lattice overtones, and two bands (804 and 463 cm^{-1}) associated to symmetric stretching and bending of Si–O bonds, respectively. There is a significant change with the band at approximately 600 cm^{-1}, associated to SiO_4 tetrahedrons, present in the sample before hydrothermal treatment but gone after the treatment, in an indication of loss of structural order.

3.3. BET analysis

Fig. 3 shows the nitrogen adsorption–desorption isotherms at 77 K of the MCM-41 materials, before and after hydrothermal treatment at 450 °C. All the isotherms have a sharp inflection at a relative pressure about 0.36 which is characteristic of capillary condensation within uniform mesopores. This capillary condensation in the nitrogen adsorption curve was observed between 0.3 and 0.4 p/p_0 at 392 MPa pressure.

Table 1 shows the nitrogen sorption data of Ti containing samples compared with the pure siliceous samples. The sample with Ti has lower surface specific area and smaller pore diameter, however, it has thicker walls. The MCM-41 lattice, calculated with $a_0 = 2d_{1\,0\,0}/\sqrt{3}$, was of 41 Å and after thermal treatment it became of 29 Å.

The pore volume decreased from 0.90 to 0.50 cm^3/g for the MCM-41 sample, and from 0.78 to 0.64 cm^3/g in the Ti-MCM-41 sample. The BET specific surface area of MCM-41 also decreased from 1400 to 950 m^2/g and 800 m^2/g after the hydrothermal treatment at 450 and 550 °C (32% and 43% reduction, respectively), whereas, for the Ti-MCM-41 material, there was a reduction of specific surface area of 12% and 19%, respectively. The breaking of the structure and the formation of an amorphous SiO_2 phase having low surface area may explain the reduction of the specific surface area of the samples.

Although there was a reduction of pore size, pore volume and specific surface area for both materials, this reduction was smaller for the Ti-containing MCM-41, indicating that the thicker walls provided more stability. The same observation can be noticed in Fig. 3. The nitrogen adsorption-desorption isotherms of Ti-MCM-41 before and after hydrothermal treatment are closer to each other as compared with the MCM-41 isotherms [14,15]. Before hydrothermal treatment, MCM-41 and Ti-MCM-41 isotherms are close to each other, whereas after hydrothermal treatment there is a considerable separation between the isotherms and the order became inverted.

Table 1
Textural properties of MCM-41 and Ti-MCM-41 samples before and after hydrothermal tests

Sample	S_{BET} (m^2/g)	a_0 (Å)	V_{mp} (cm^3/g)	d_p (Å)	Wall thickness (Å)
MCM-41	1400	41.0	0.90	25.8	17.3
MCM-41 (450)	950	30.9	0.75	20.6	10.4
MCM-41 (550)	800	29.0	0.50	19.2	10.2
Ti-MCM-41	1200	43.5	0.78	22.7	19.8
Ti-MCM-41 (450)	1050	37.7	0.67	20.6	11.5
Ti-MCM-41 (550)	970	35.0	0.64	20.0	11.0

3.4. Thermogravimetric analysis

TGA analysis of MCM-41 materials exhibits distinct weight losses that depend, in part, on the composition of the sample [15,16]. The TGA and DTA plots of MCM-41 are shown in Fig. 4a and b. The TGA/DTA curves of Ti-MCM-41 were very similar. The as synthesized material has approximately 50% of the MCM-41 phase; the remaining part corresponds to water and organic components. The mass loss is related to the following stages, consistent with the enthalpy changes observed by DTA: (1) desorption of water before 100 °C, (2) decomposition of the surfactant between 145 and 280 °C, (3) breaking of the hydrocarbon chain between 280 and 320 °C, (4) combustion of remaining

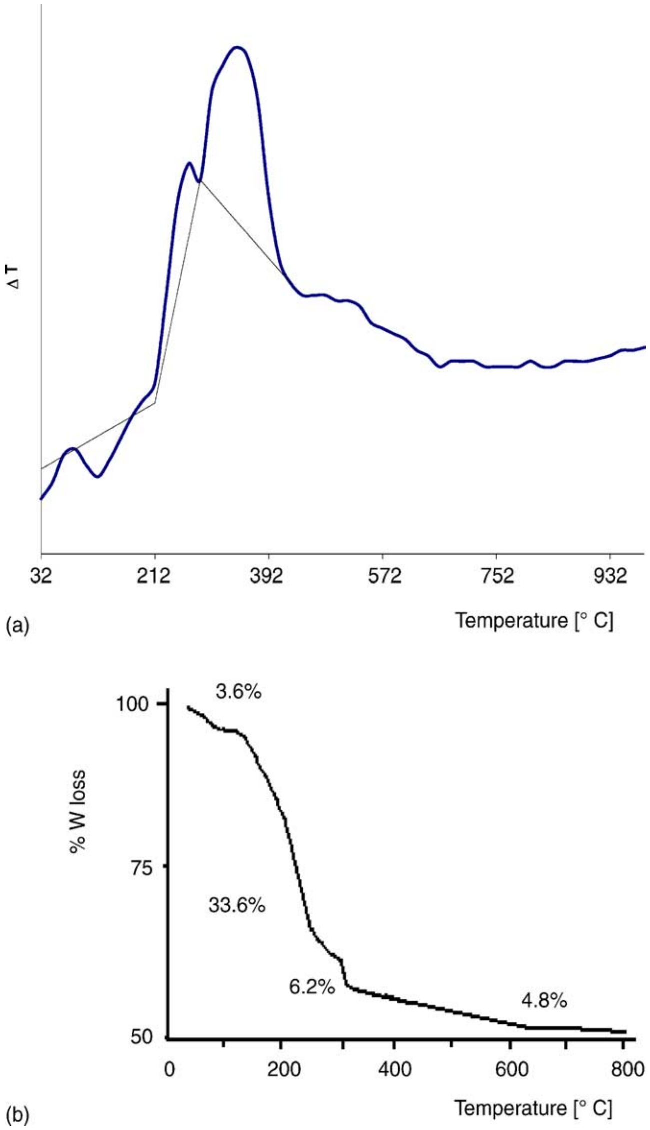

Fig. 4. (a) TGA curve and (b) DTA curve of the MCM-41 sample.

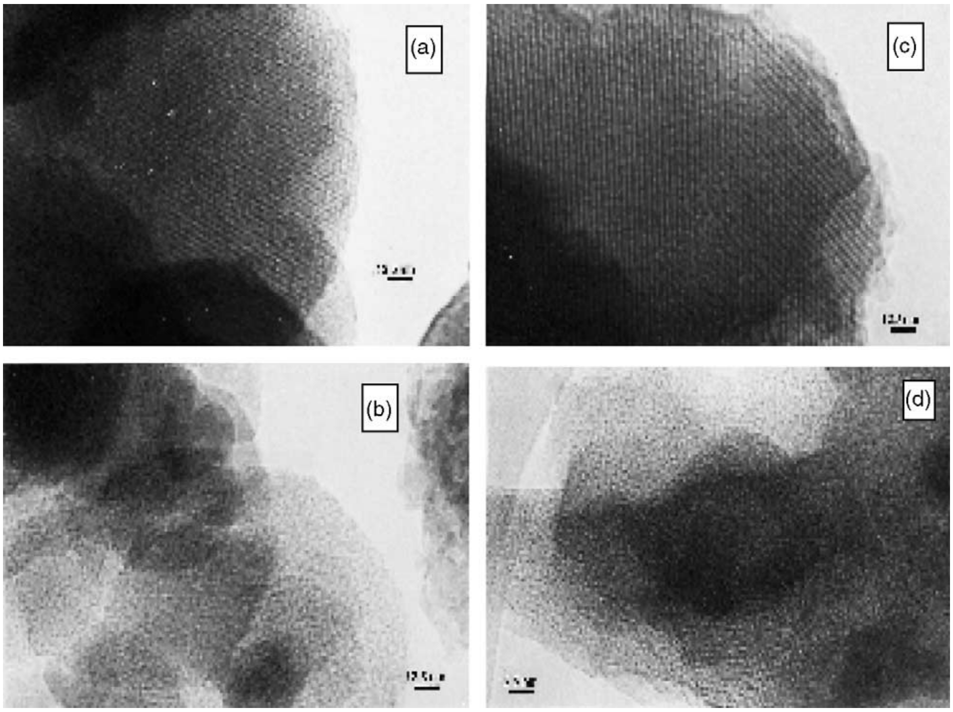

Fig. 5. TEM micrographs of MCM-41 (a) before and (b) after hydrothermal treatment at 550 °C, and Ti-MCM-41 (c) before and (d) after hydrothermal treatment at 550 °C.

organic species, (5) dehydroxylation and water loss associated to condensation of silanol groups between 320 and 620 °C.

3.5. Transmission electronic microscopy

Transmission electron micrographs of the MCM-41 and Ti-MCM-41 samples show a regular hexagonal array of uniform channels (Fig. 5a and c). The pores are seen to be arranged within layered material sections formed by regular rows approximately 800 Å long. After hydrothermal treatment at 550 °C, the pore array becomes more irregular and less geometric (Fig. 5b and d). EDX results of the elemental composition of the Ti-MCM-41 sample before and after hydrothermal treatment are shown in Fig. 6a and b. There are tow peaks of Au and Pd, used for coating the samples with a conductive layer and there are two Ti peaks that remain after hydrothermal treatment, in agreement with IR results. EDX mapping of the Ti-MCM-41 sample after hydrothermal treatment confirms the presence of titanium uniformly distributed within the framework (Fig. 7).

3.6. Catalytic evaluation

Table 2 shows the conversion and products obtained in the hydrodesulfurization reaction of DBT and DBT derivatives. The Ti-MCM-41 supported catalyst had a 27% higher DBT conversion and a higher proportion of biphenyl and phenylciclohexane products, whereas for the MCM-41 supported catalyst there was a higher proportion of bicyclohexyl, related to a more hydrogenating ability. FT-IR pyridine adsorption determinations (not shown) indicate that the Ti-MCM-41 sample has a larger proportion of Lewis

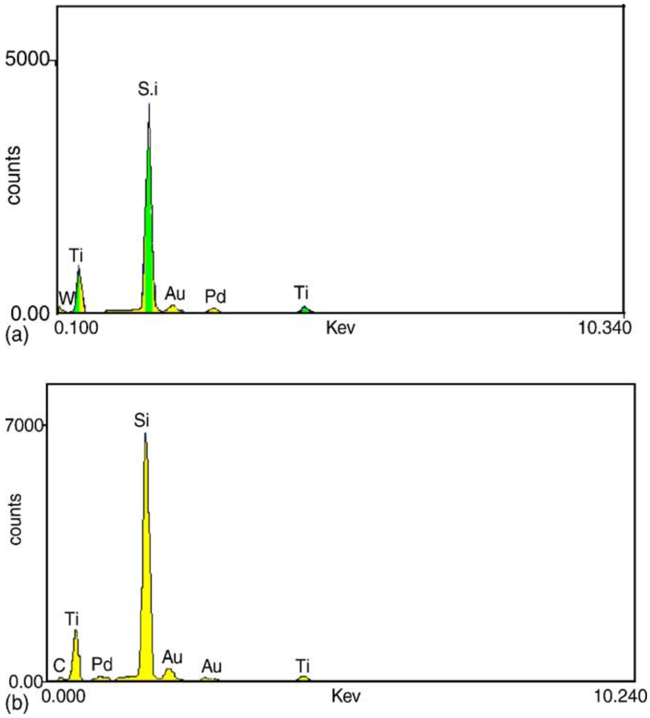

Fig. 6. Approximate elemental composition of the Ti-MCM-41 material determined by EDS (a) before and (b) after hydrothermal treatment.

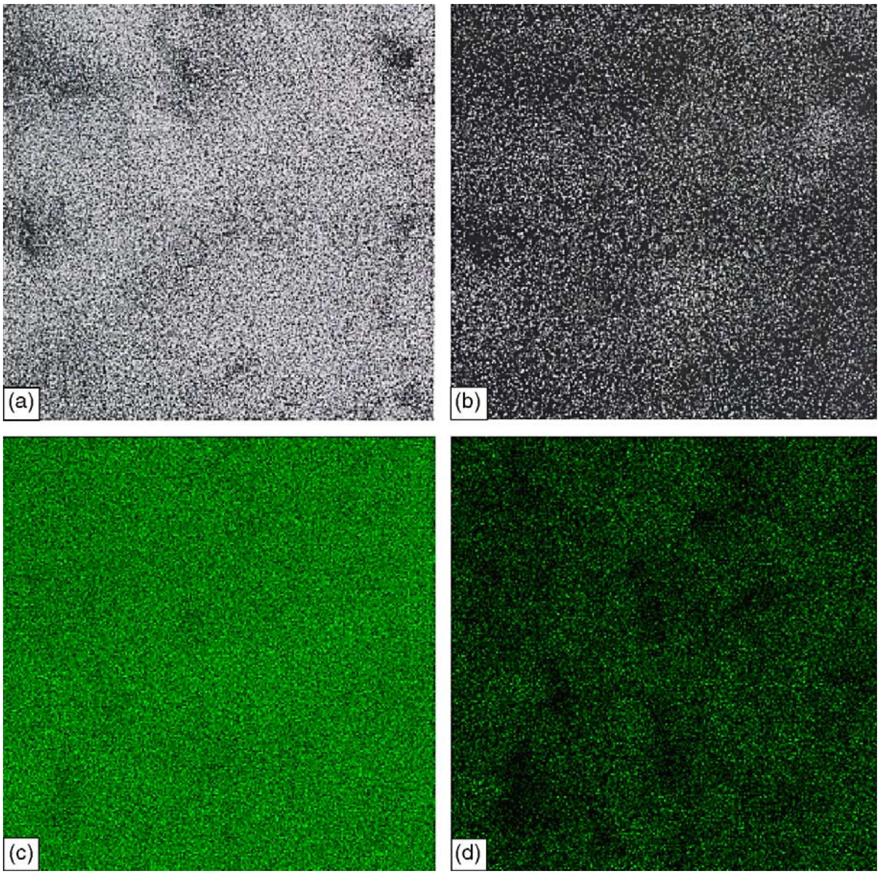

Fig. 7. Si and Ti EDS mapping of the Ti-MCM-41 sample: (a) Si distribution and (b) Ti distribution before hydrothermal treatment, (c) Si distribution and (d) Ti distribution after treatment.

Table 2
Catalytic performance for the HDS reaction of DBT over CoMo/MCM-41 and CoMo/Ti-MCM-41

	Feed (mol%)	CoMo/MCM-41	CoMo/Ti-MCM-41
n-Hexadecane[a]	95.51	–	–
Dibenzothiophene (DBT)	2.41	1.34	1.05
Others (R-DBT)[b]	2.08	0.76	0.75
Biphenyl (BP)	–	0.91	1.09
Phenylcyclohexane (PCH)	–	0.01	0.33
Bicyclohexyl (BCH)	–	0.22	0.03
DBT conversion (%)	–	44.4	56.4
Others (R-DBT) conversion %	–	63.46	63.94

[a] Solvent.

[b] Alkyl-DBT, reaction conditions: 300 °C, 400 psig, 9.0 h^{-1} WSHV, 2.0 h time.

acid sites than the MCM-41 sample. Bicyclohexyl and phenylcyclohexane are obtained *via* a hydrogenation reaction, favored by Bröensted acid sites, whereas, the biphenyl product is obtained via a direct desulfurization path, favored by Lewis acid sites.

Conversion results are consistent with previous works, carried out with the TiO_2–Al_2O_3 system for HDS reactions [17,18] that have reported that TiO_2-containing catalysts are more catalytically active and present polymolybdenum structures with octahedrally coordinated Mo, which are considered precursors of the MoS_2 active phase.

4. Conclusions

The introduction of heteroatoms, such as Al, in the MCM-41 framework, usually reduces the thermal and hydrothermal stability of the material. However, in the case of the present investigation, the samples containing Ti had thicker walls that improved the hydrothermal stability.

The hydrothermally treated siliceous MCM-41 material presented losses of BET specific surface area of approximately 42% and of primary mesoporous volume of 44%. In contrast, the hydrothermally treated Ti-MCM-41 material presented losses of specific surface area of 20% and losses of primary mesoporous volume of 18%. Therefore, the Ti-MCM-41 sample has better resistance to hydrothermal treatment. IR results showed that the Ti remains part of the framework while there is a loss of structural order.

The Ti-MCM-41 material also had a better catalytic performance; it is considered that TiO_2 favors the formation of the MoS active phase.

Acknowledgements

We acknowledge the financial support from the IMP-FIES program and the technical support of Ricardo Ramírez.

References

[1] B. Delmon, G.F. Froment, P. Grange, Hydrotreatment Hydrocrack. Oil Fract. 153 (1999) 397–401.

[2] G. Marroquín, J. Ancheyta, A. Ramírez, E. Farfán, Energy Fuels 15 (2001) 1213–1219.

[3] M.L. Occelli, S. Biz, A. Auroux, Appl. Catal. A 183 (1999) 231–239.

[4] J.S. Beck, US Patent 5,057,296 (1991).

[5] V. González-Peña, I. Díaz, C. Márquez-Alvarez, E. Sastre, J. Pérez-Pariente, Micropor. Mesopor. Mater. 44/45 (2001) 295–302.

[6] F. Díaz Mohino, J. Pérez-Pariente, E. Sastre, Appl. Catal. A 205 (2001) 19–30.

[7] C.Y. Chen, H.X. Li, M.E. Davis, Micropor. Mater. 2 (1993) 17.

[8] L.Y. Chen, S. Jaenicke, G.K. Chuah, Micropor. Mater. 12 (1992) 323.

[9] N.Y. He, S.L. Bao, Q.H. Xu, Stud. Surf. Sci. Catal. 105 (1997) 85.

[10] A. Corma, M.T. Navarro, J. Perez Pariente, J. Chem. Soc. Chem. Commun. 147 (1994).

[11] (a) L. Noreña-Franco, I. Hernandez-Perez, J. Aguilar-Pliego, A. Maubert-Franco, Catal. Today 75 (2002) 189–195;
(b) L. Norena, M.Sc. Thesis, UMIST, UK, 1993.

[12] J.S. Lee, C.H. Rhee, Catal. Today 38 (1997) 213–219.

[13] N. He Zlu, C. Yuan, J. Hong, C. Yang, S. Bao, Q. Xu, Supramol. Sci. 5 (1998) 553.

[14] G. Gu, P.P. Ong, C. Chu, J. Phys. Chem. Solids 60 (1999) 943.

[15] M. Busio, J. Janchen, J.H.C. Van Hooff, Micropor. Mater. (1995) 211–218.

[16] R.B. Borade, A. Clearfield, in: M.L. Occelli, H. Kessler (Eds.), Synthesis of Materials: Zeolites, Clays and Nanostructures, Marcel Dekker Inc., New York, 1997.

[17] Z.B. Wei, W. Yan, H. Zhang, T. Ren, Q. Xin, Z. Li, Appl. Catal. A 167 (1998) 39.

[18] J.R. Grzechowiak, J. Rynkowski, I. Wereszczako-Zielinska, Catal. Today 65 (2001) 225.